

# Jointly Iterative Decoding of Low-Density Parity Check codes (LDPC) coded Continuous Phase Modulation (CPM)

Zhang Nan, Gao Xiao and Xu Ye-mao

Wuhan Maritime Communication Research Institute, Wuhan, 430079, China

nan\_zhang313@sina.com, gaoxiao1113@sina.com

**Abstract**—This paper investigates the performance of a Low-Density Parity Check codes (LDPC)-coded system transmitted over A WGN channels using octal partial response Continuous Phase Modulation (CPM). The system provides an attractive option for spectral efficient communications systems. The CPM modulator can be decomposed into a ring continuous-phase encoder (CPE) followed by a memoryless modulator (MM), where the CPE is as the same algebra as convolutional code. With a pragmatic approach, The LDPC codes are designed through the use of the proposed analysis technique based on extrinsic information transfer (EXIT) charts. We propose a belief propagation (BP)-based iterative decoding algorithm at the receiver. The hybrid design combined with iterative decoding yield very good performances compare with the conventional communication schemes. The results show the considerable superiority of the iterative algorithm.

**Index Terms**—component, LDPC codes, CPM, iterative decoding, extrinsic information transfer (EXIT) charts.

## I. INTRODUCTION

LOW-density parity-check (LDPC) codes have attracted considerable attention in the coding community because they can achieve near-capacity performance with iterative message-passing decoding and sufficiently long block sizes. For example, in [1], Chung et al. presented a block length 107 (ten million bits) rate-1/2 LDPC code that achieves reliable performance—a 10<sup>-6</sup> bit error rate (BER)—on an additive white Gaussian noise (AWGN) channel with a signal-to-noise ratio (SNR)  $E_b / N_0$  within 0.04 dB of the Shannon limit.

Continuous phase modulation (CPM) is a class of phase modulated signals with constant envelope and spectral occupancy that can be tailored to any available bandwidth. Due to its good spectral properties and ability to allow nonlinear amplifiers to be operated in saturation, continuous phase modulation (CPM) is widely used on radio channels. CPM by itself is a form of coded modulation due to the memory created by the continuous phase of the signal and possibly by the additional memory introduced by partial response signaling (a scheme used here). Rimoldi in [2] showed that a CPM can be decomposed into a continuous phase encoder (CPE) and a memoryless modulator (MM). The CPE operates over a ring of integers, which are not necessarily binary, producing codeword sequences that are mapped onto waveforms by the MM, creating a continuous phase signal. Once the memory of CPM

is made explicit, it is possible to design a coded CPM system [3, 6, 7] by combining the LDPC code and the CPE into a single joint LDPC-convolutional code (Table I). Systems designed in this manner typically have larger Euclidean distances and thus perform better than systems designed using the traditional approach.

The rest of the paper is organized as follows. Section II describes the model of LDPCC-CPM system. Section III we introduce the EXIT chart-based analysis of the iterative algorithm. Section IV introduces the proposal of CPM. Simulations are discussed in section V. Finally, we conclude the paper in section VI.

## II. SYSTEM DESCRIPTION

As shown in [2], any CPM scheme can be divided into a continuous phase encoder (CPE) and a memoryless modulator (MM). Using the memorial and recursive character of CPE, combined with LDPC code and interleaver outside, the model of LDPCC-CPM system is founded.

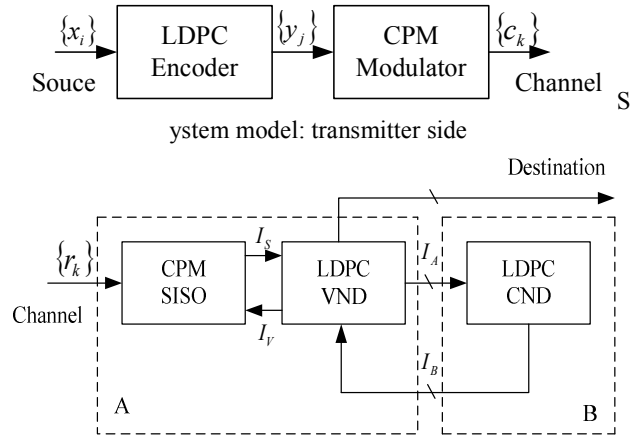


Figure 1. System model: receiver side

The transmitter scheme, shown in Fig. 1, consists of a simple concatenation of an outer LDPC encoder and an inner CPM modulator, which is directly connected to the channel. Without loss of generality, we consider the discrete-time lowpass equivalent model of the communication system. A

binary sequence  $\{x_i\}$  at the input of the LDPC encoder is coded into a binary sequence  $\{y_j\}$  (representing a codeword). The binary symbols  $\{y_j\}$  are then coded and mapped to high-order modulated symbols  $\{c_k\}$ .

TABLE I.  
PREVIOUS WORK ON CORELATIVE SCHEME

Code ID	Rate	Reference
(2048, 3, 6) LDPC-CC	1/2	[23]
(100000, 3, 6) LDPC-CC	1/2	[24]
(256, 3, 8) LDPC-CC	5/6	[22]
Extended BCH CPM	1/2	[21]
LDPC-CPM(L=2)	1/2	[18]

The receiver is depicted in Fig. 2. At the input of the receiver, the sequence of channel observations is denoted as  $\{r_k\}$ . For simplicity, we are considering one sample per coded symbol. If two or more samples per symbols are necessary, such as to allow for a time varying channel, the proposed derivation can be extended by considering a suitable vector notation.

The receiver is partitioned into two blocks, denoted as block  $A$  and block  $B$ . Block  $A$  comprises the following subblocks.

- A SISO block matched to the CPM and the channel, and referred to as CPM-SISO block. This block computes the a posteriori reliabilities of the binary symbols  $\{y_j\}$  at the input of the receiver on the basis of the channel observations and the relevant a priori reliabilities (coming from the block labeled “LDPC VND” and described below).
- An LDPC variable node detector (VND), associated with the variable nodes in the code bipartite graph. This block computes the reliability of each binary symbol  $y_j$  based on the reliabilities from the CPM-SISO block and the information received from block  $B$  and based on the code constraints.

Block  $B$  includes the LDPC check node detector (CND), associated with the check nodes in the code bipartite graph. The LDPC CND computes the reliability of each binary symbol  $y_j$  based on the a priori reliabilities received from the LDPC VND and based on the LDPC code constraints. The reliabilities at the output of block  $A$  are computed as follows.

- 1) The VND processes the messages coming from block  $B$  by performing, at each variable node, a sum of all the incoming messages excluding the one coming from the CPM-SISO block. The obtained messages are passed to the CPM-SISO block as a priori input.

- 2) The CPM -SISO block computes, based on the observations from the channel and the a priori information, reliability values according to its internal algorithm.
- 3) Finally, the VND computes the messages to be sent to block  $B$  according to the standard LDPC decoding algorithm, but using, as a priori input, the messages from the CPM -SISO decoder.

It is important to note that, in all the above computations, only the so-called extrinsic information is exchanged between the component blocks [8], [9]. The overall decoding algorithm at the receiver can be described as follows.

- As initialization step, the a priori reliabilities of the symbols  $\{y_j\}$  at the input of block  $A$  (from block  $B$ ) correspond to complete uncertainty (a value equal to 0 in the LL domain).
- Decoding starts from block  $A$ , which computes output reliabilities and sends them to block  $B$ . At the first step, since all the messages coming from the CND are 0, the output of block  $A$  simply consists of the output of the CPM-SISO.
- The LDPC CND (i.e., block  $B$ ), thus, computes the extrinsic information to be passed to block  $A$ .
- The algorithm iterates from the second step until a valid LDPC codeword is obtained or a maximum number of  $N_i$  iteration have been performed.
- In the case a valid LDPC codeword is not obtained, an additional standard LDPC decoding algorithm is applied based on the last extrinsic information at the input of LDPC VND block. This corresponds to iterating information only between LDPC VND and LDPC CND. The maximum number of standard LDPC decoding iterations is  $N_{LDPC}$ .
- At the end of the process, the complete (not extrinsic) reliabilities are computed by the LDPC VND and delivered to the destination.

### III. EXIT CHARTS AND ITERATIVE DECODING

#### A. Degree Distributions

The degree distributions of an LDPC code are polynomials denoted as  $\lambda(x)$  and  $\rho(x)$ , whose coefficients  $\{\lambda_i\}$  and  $\{\rho_j\}$  correspond to the fraction of branches in the graph connected to degree- variable nodes and degree- check nodes, respectively, [5]. The polynomial  $\rho(x)$  is defined as the check node degree distribution and  $\lambda(x)$  is defined as the variable node degree distribution. The coefficients  $\{\rho_j\}$  and  $\{\lambda_i\}$  must satisfy the following constraints [5]:

$$\begin{aligned}
0 &\leq \rho_j \leq 1 & j \geq 1 \\
0 &\leq \lambda_i \leq 1 & i \geq 1 \\
\sum_{j=1}^{\infty} \rho_j &= 1 \\
\sum_{i=1}^{\infty} \lambda_i &= 1
\end{aligned} \tag{1}$$

Moreover, the following linear constraint must be satisfied for a degree distribution in order to be compatible with a given code rate  $R$  [5]:

$$\sum_{j=1}^{\infty} \frac{\rho_j}{j} = (1-R) \sum_{i=1}^{\infty} \frac{\lambda_i}{i} \tag{2}$$

### B. EXIT Chart-Based Analysis of the Receiver Performance

For each block shown in Fig. 2, it is possible to draw the corresponding EXIT curve [10], [11]. In Fig. 2, the MI at the output of each block  $A$  and  $B$  is denoted as  $I_A$  and  $I_B$ , respectively; within block, the MI at the input and output of the CPM-SISO subblock are labeled  $I_V$  and  $I_S$ , respectively. The decoding process can then be represented as a recursive update of the MI in the EXIT charts. If the MI converges to 1, it is possible to predict that the BER will converge to zero.

At this point, we are interested in the computation of the EXIT charts of blocks  $A$  and  $B$ . Block is simply characterized by the EXIT curve of the LDPC VND, while the EXIT curve of block  $A$  is obtained by combining the EXIT curve of the LDPC VND with that of the CPM-SISO block. In [12], some formulas are given for the computation of LDPC VND and LDPC VND EXIT curves on the basis of a Gaussian assumption for the exchanged messages, which provides great simplification and good accuracy. Since, in general, the analytical computation of the CPM-SISO EXIT curve is a difficult task, approximate computation can be based on Monte Carlo simulations [12].

In the following, approximate formulas are given for the EXIT curves  $I_A$  (of block  $A$ ) and  $I_B$  (of block  $B$ ) [12]:

$$I_B = 1 - \sum_j \rho_j J(\sqrt{j-1} J^{-1}(1-I_A)) \tag{3}$$

$$I_A = \sum_j \lambda_i J(\sqrt{(i-1)(J^{-1}(I_B))^2 + (J^{-1}(I_S))^2}) \tag{4}$$

where the function  $J(\cdot)$  is defined as follows:

$$J(\sigma) = \int_{-\infty}^{+\infty} \frac{1}{\sqrt{2\pi\sigma^2}} e^{-\frac{(x-\frac{\sigma^2}{2})^2}{2\sigma^2}} \log_2 \frac{2}{1+e^{-x}} dx \tag{5}$$

The MI  $I_S$  at the output of the CPM-SISO block is a function of the MI  $I_V$  of the messages passed by the VND to the CPM-SISO block and corresponds to the EXIT function of

the CPM-SISO. The MI  $I_V$  of the messages passed by the LDPC VND to the CPM-SISO block can be approximately computed as follows [12]:

$$I_V = \sum_i \lambda_i J(\sqrt{i} J^{-1}(I_B)) \tag{6}$$

### C. Optimizing the EXIT Charts

In [5], it is shown that by “eye fitting” the two EXIT curves  $I_A(I)$  and  $I_B^{-1}(I)$  by varying the degree distributions  $(\lambda(x), \rho(x))$ , a significant system performance improvement can be obtained. Since the EXIT curves of VND and VND, relative to the most powerful known LDPC codes for memoryless channels, are very similar at “pinch-off”, i.e., when EXIT curves touch, and considering the good results obtained in [12], at a first glance fitting the EXIT curves seems a good optimization strategy. However, if only low degree nodes are allowed, this similarity of curves becomes less noticeable and usually “low degree only” distributions are desirable in order to keep the LDPC code parity-check matrix as sparse as possible [4], [5]. Moreover, it is important to note that, given a particular signal-to-ratio (SNR), convergence of the decoding process can be obtained if the tunnel between the two curves is open. Hence, our actual goal, while performing optimization, is to keep the tunnel open. Our optimization algorithm is based on a simple random walk in the degree distribution parametric space. Before describing how this algorithm works, we first provide the reader with some useful considerations and definitions.

Consider, first, two couples of EXIT curves for blocks  $A$  and  $B$ , denoted as  $(I_{1,A}(\cdot)I_{1,B}^{-1}(\cdot))$  and  $(I_{2,A}(\cdot)I_{2,B}^{-1}(\cdot))$ , respectively. It can be easily verified that if

$$\begin{aligned}
I_{1,A}(I) &\geq I_{2,A}^{-1}(I) & \forall I \in (0,1) \\
I_{1,B}^{-1}(I) &\geq I_{2,B}^{-1}(I) & \forall I \in (0,1)
\end{aligned} \tag{7}$$

i.e.,  $I_{1,A}$  is higher than  $I_{2,A}$  and  $I_{1,B}^{-1}$  is lower than  $I_{2,B}^{-1}$ , then the convergence of the decoding process for the system relative to the EXIT curves  $(I_{1,A}(\cdot)I_{1,B}^{-1}(\cdot))$  will not be slower than the convergence of the system relative to the EXIT curves  $(I_{2,A}(\cdot)I_{2,B}^{-1}(\cdot))$ .

It should be observed that the two EXIT curves touch at point  $(1,1)$ —a sufficient condition for this is the absence of degree-1 variable nodes in the code, as it can be easily seen by imposing  $\lambda_1 = 0$  in (3) and letting  $I_B \rightarrow 0$ . The iterative decoding algorithm for a system characterized by the EXIT curves  $(I_A(\cdot), I_B^{-1}(\cdot))$  cannot converge if there exists a value  $I^*$ ,  $0 < I^* < 1$ , such that  $I_A(I^*) < I_B^{-1}(I^*)$ , i.e., the tunnel is closed. We then need to define a functional representative of the tunnel closure: the more the tunnel is closed, the lower this functional must be. A possible choice is the following:

$$f(\lambda, \rho) = \min_{I \in [0,1]} \{I_A(I) - I_B^{-1}(I)\} \quad (8)$$

where we have explicitly indicated the dependence of the functional on the degree distributions. Since, as previously observed, the EXIT curves touch at (1,1), this functional cannot be positive. Moreover, this functional depends also on the particular channel as well as on the CPM-SISO block. As previously observed, it is reasonable to assume that increasing the SNR raises the EXIT curve of block  $A$ , while decreasing the SNR lowers it. In other words, if the tunnel between the two EXIT curves is at pinch-off, a small SNR increment should be sufficient to open it.

The design parametric space is given by the node degree distributions  $\{\rho_j\}$  and  $\{\lambda_i\}$ . According to (1) and (2), three parameters are linearly dependent on the others. Hence, one has to choose a parameter from the set  $\{\lambda_i\}$ , a parameter from the set  $\{\rho_j\}$ , and an additional parameter from either  $\{\lambda_i\}$  or  $\{\rho_j\}$ . The chosen parameters have then to be expressed as functions of the remaining free parameters. There is no constraint on the numbers of elements of the sets  $\{\lambda_i\}$  and  $\{\rho_j\}$ , provided that these sets are not empty, contain at least four elements and are finite.

We now describe the proposed optimization algorithm. We start with given valid degree distributions associated to a given code rate, according to (2), and determined by a tuple of free parameters. If the tunnel is not closed, i.e.,  $f(\lambda, \rho) = 0$ , we decrease the SNR until the tunnel closes and  $f(\lambda, \rho) < 0$ . New tuples of free parameters are then obtained, by repeatedly adding to the previous tuple a Gaussian increment until all inequalities in (1) are satisfied. The mean of the Gaussian increment is zero and the standard deviation is used to “tune” the optimization algorithm. From the new tuple, we evaluate  $\lambda(x)$  and  $\rho(x)$  and, consequently, the value  $f(\lambda, \rho)$ : if this value is larger than the previous one, we substitute the previous tuple with the new one. If the tunnel opens, the SNR is decreased again, and previous steps are repeated. The algorithm stops when a specific requirement is met, such as, for example, the obtained code ensemble corresponds to an EXIT chart with an open (not closed) tunnel for a desired SNR, or a maximum number of steps (in the random walk) is reached. The steps of the proposed optimization algorithm are summarized in Table II. As a possible improvement for the optimization algorithm, one can diminish the step value, i.e., the standard deviation of the Gaussian increment vector, after a given number of unsuccessful trials. Unlike the EXIT curve fitting optimization algorithm in [12] and [13], the proposed technique offers the advantage of being effective also for small sets of possible node degrees.

TABLE II.  
ALGORITHM: BASIC STEPS

<b>Start Initialize <math>\lambda(x)</math> and <math>\rho(x)</math> and compute <math>f(\lambda, \rho)</math>.</b>	
1	While tunnel is open reduce SNR by small steps and compute the final value of $f(\lambda, \rho)$ .
2	Find a new $(\lambda', \rho')$ compatible with code rate at random distance from $(\lambda, \rho)$ .
3	Compute new $f(\lambda', \rho')$ ; if not larger than previous $f(\lambda, \rho)$ goto step 2, else $(\lambda, \rho) \leftarrow (\lambda', \rho')$ .
4	If stop condition is not reached goto 1 else output $(\lambda, \rho)$ and final SNR.

The proposed algorithm basically performs an optimization of the convergence threshold, defined as the lowest SNR such that the tunnel is open. Within the approximation of the EXIT chart-based analysis, the decoding process converges above this SNR threshold. The simplicity of the proposed optimization algorithm enables a joint optimization of both  $\lambda(x)$  and  $\rho(x)$  in the presence of the CPM-SISO block.

#### IV. SIMULATION RESULTS AND COMPARISON

In order to test the validity of the iterative detection method, we employed Monte Carlo simulations to evaluate the performance of the proposed system over an A WGN channel. Then the effect of LDPC code length and iterative number on the performance of the system is studied. In simulations, all the LDPC codes have lower triangular parity check matrix, and the iterative encoding algorithm is adopted and the number of iterations is 8. Table III and Table IV shows more details of the CPM and LDPC. In CPM modulator, we employed  $g(t)$  with pulse length  $L=3$ . This scheme will be denote as 3RC.  $M$  is taken to be 8 in this study since this easily fits the encoder structure in addition to the high rate it brings along. The modulation index  $h$  is arbitrarily fixed at  $1/2$ .

TABLE III.  
PARAMETERS OF CPM

Modulation Index	H=1/2
Correlation Length	L=3
Phrase Pulse	RC

TABLE IV.  
PARAMETERS OF LDPC CODES

Check matrix	Code rate	Girth	Degree distribution
(192,384)	1/2	8	$\lambda(x) = 0.25x + 0.75x^2$
(384,768)			
(540,1080)			
(768,1536)			

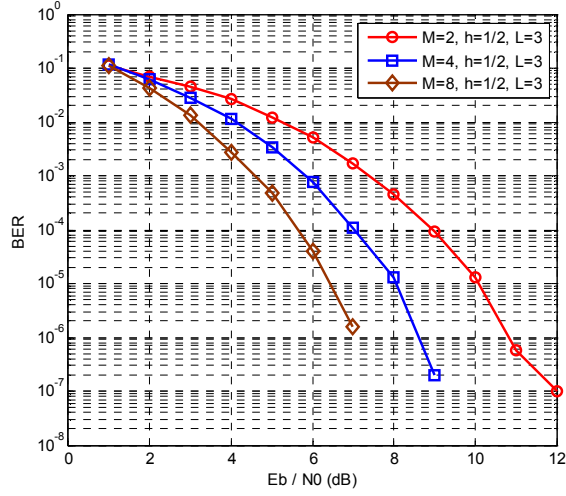


Figure 2. BER performance of  $M$ -ary ( $M=2,4,8$ ) CPM

Fig. 3 shows BER for  $M$ -ary CPM with 3REC pulse respectively. As we see from Fig. 3 BER performance is improved with the increasing of  $M$ . In order to deliver the information reliably, we select  $M=8$ ,  $L=3$ ,  $h=1/2$ . Theoretic analysis and simulation results in A WGN show that the 8M3RC scheme is a good choice to achieve high-speed transmission.

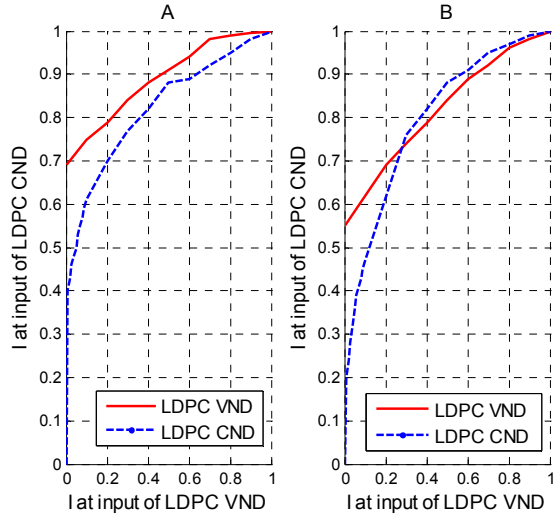


Figure 3. EXIT chart-based analysis of a system with serial concatenation of an LDPC code and CPM. (a) EXIT chart of rate 1/2 regular LDPC code concatenated with CPM ( $E_b/N_0 = 2.5$  dB). (b) EXIT chart of an optimized rate 1/2 LDPC code concatenated with CPM ( $E_b/N_0 = 0.8$  dB)

In Fig. 4(a), EXIT charts are shown for a regular rate-1/2 LDPC code, characterized by  $\lambda(x) = x^2$  and  $\rho(x) = x^5$ . We preliminarily observe that the use of this code, mapped to a CPM modulation format, represents a good tradeoff between complexity and performance for transmission over an AWGN channel. The EXIT curves are computed at

$E_b/N_0 = 2.5$  dB: the dotted curve is the EXIT curve of block  $B$  (LDPC CND). Note that the SNR does not influence the EXIT curve relative to the LDPC CND (the dotted one in Fig. 4). It is easy to see that the system is at pinch-off: convergence at this and lower values of  $E_b/N_0$  is not possible. The solid curve represents the EXIT curve of the LDPC VND: this corresponds to the CPM system, i.e., LDPC BICM. It can be immediately seen that at  $E_b/N_0 = 2.5$  dB the tunnel, relative to a transmission scheme is open. The EXIT chart-based analysis then predicts that, for a bit SNR slightly lower than 2.5 dB, the system does not converge.

Fig. 4(b) shows the EXIT curves for this optimized code ensemble for  $E_b/N_0 = 0.8$  dB: the curves correspond to block  $B$ . It is immediate to recognize that the tunnel is at pinch-off. The solid curve in Fig. 4(b) is the EXIT curve of the LDPC VND: the tunnel is “heavily” closed, predicting that the system with CPM should perform significantly better than the single LDPC code without CPM. Note that the convergence SNR threshold predicted by the results in Fig. 4(b) is around 0.9 dB

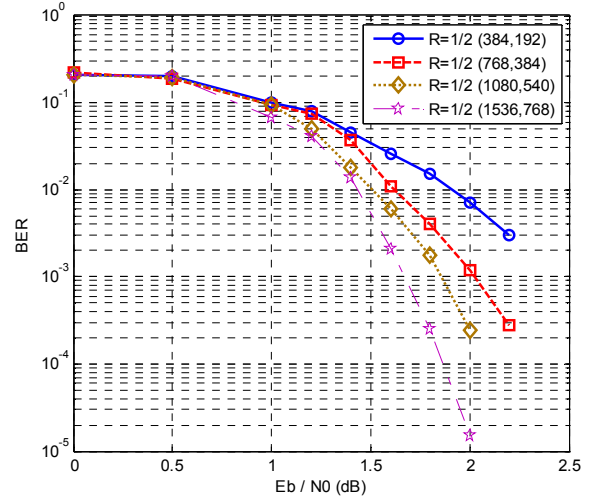


Figure 4. BER performance of LDPC-CPM with various code length

Fig. 5 shows the BER performance of LDPC-8M3RC scheme with different code length. It is obvious that the BER performance is improved substantially by increasing the length of LDPC code for fixed code rate. As we see from Fig. 4, a BER of  $1.45 \times 10^{-5}$  is attainable at an  $E_b/N_0$  of 2 dB using long code length 1536 bits. Furthermore, the code length is not too long to implement with temperate complexity.

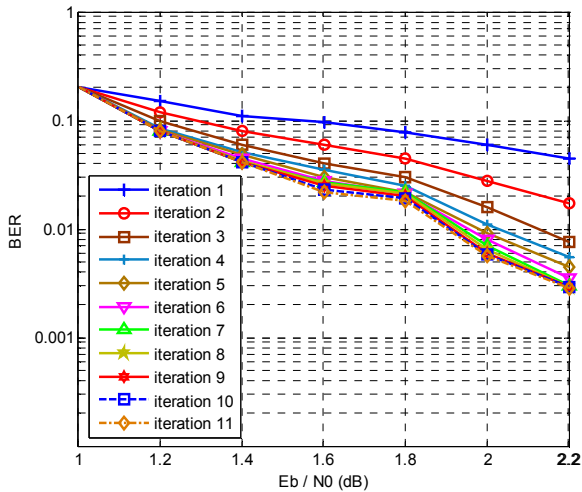


Figure 5. BER performance of LDPC-CPM with various iterations

Fig. 6 shows the BER performance of LDPC-8M3RC for various iterations with information block length 192 bits and code rate 1/2. As we see from Fig. 6, BER descends with the increasing number of iteration and tends to be stable. Iterations have little influence on performance improvement in the region of 0.5-1.0dB, while the BER performance is improved rapidly with the increase of the number of iteration when  $E_b/N_0$  is higher than 1.0 dB. The gain of iteration is very small after 6 times iterations. In order to reduce iterative decoding delay and complexity of hardware, the number of iteration is set to 8.

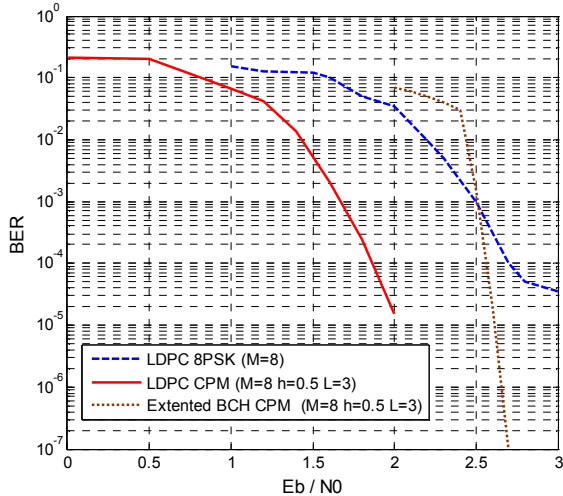


Figure 6. Performance of a LDPC-CPM, LDPC-8PSK and BCH-CPM

To assess the performance of the proposed LDPC-CPM scheme over previous LDPC based systems and CPM based system. The proposed system is compared with other schemes, where a regular LDPC systematic code of rate  $R = 1/2$  and block length  $K = 1536$  is used for the systematic code. As shown in Fig. 7, for  $BER = 10^{-6}$  the proposed LDPC-8CPM-

3RC scheme is 0.8dB better than extended BCH-coded 8CPM-3RC system, extended BCH-codes have been shown in [14] to be very effective in CPM schemes. Furthermore LDPC-CPM scheme exhibit lower “error floor”.

We have presented an unequal error-protection scheme based on LDPC coded CPM. With focus on EXIT of LDPC, we have derived an interactive algorithm for symbol detection over AWGN channels. Also, we have presented a practical coding scheme that can be good performance compare with other schemes. From the above-mentioned simulations, we easily see that the iterative detection method could effectively improve the BER performance in narrow band and low SNR environment. We can determine the system parameters, i.e., LDPC code length 1536 bits, code rate is 1/2, CPM signal is 8M3RC with index 1/2, and the iterative number is 8.

## V. CONCLUSION

CPM is an excellent digital modulation scheme which has constant-envelope, and is bandwidth and energy efficient. In order to obtain further improvement in energy efficiency, CPM can be combined with a LDPC code. Iterative detection based on turbo principle is an effective approach to improve the performance of LDPC-CPM system. The main advantage of the proposed scheme with respect to the existing superposition-coded linear modulations consists of the constant-envelope signal, so that the system does not rely on the presence of expensive amplifiers. It is shown that our proposed systems provide significant amount of coding gains over BCH coded CPM system. Furthermore, since 8M3RC scheme is selected as modulator, our system has also bandwidth efficiency. Thus, our system is very suitable for lower power and band limited applications such as satellite and mobile radio communications.

## REFERENCES

- [1] S.-Y. Chung, G. D. Forney, Jr., T. J. Richardson, and R. Urbanke, “On the design of low-density parity-check codes within 0.0045 dB of the Shannon limit,” *IEEE Commun. Lett.*, vol. 5, pp. 58–60, Feb. 2001.
- [2] B.E. Rimoldi, “A Decomposed Approach to CPW,” *IEEE Trans. Inform. Theory*, vol. 34, pp.260-270, Mar. 1988.
- [3] B.E. Rimoldi, “Design of Coded CPFSK Modulation Systems for Bandwidth and Energy Efficiency”, *IBM J. Res. Commun.*, vol. 37, pp. 897-905, Sept. 1989.
- [4] R. G. Gallager, *Low-Density Parity-Check Codes*. Cambridge, MA:MIT Press, 1963.
- [5] T. Richardson, A. Shokrollahi, and R. Urbanke, “Design of capacityapproaching irregular low-density parity-check codes,” *IEEE Trans. Inf. Theory*, vol. 47, no. 2, pp. 619–637, Feb. 2001.
- [6] R.H.-H. Ymg and D.P. Taylor, “TrelliscodedContinuous-Phase-Frequency-Shift-Key& with Ring Continuous Codes”, *IEEE T m . Inform. Theory*, vol. 40, pp. 1057-1067, July 1994.
- [7] B.E. Rimoldi and Q. Li, “Coded Continuous Phase Modulation using Ring Convolutional Codes”, *IEEE Tvans. Commun.*, vol. 34, pp. 2714-2720, Nov. 1995.
- [8] C. Berrou and A. Glavieux, “Near optimum error correcting coding and decoding: Turbo codes,” *IEEE Trans. Commun.*, vol. 44, no. 10, pp. 1261–1271, Oct. 1996.
- [9] T. Richardson and R. Urbanke, “The capacity of low-density paritycheck codes under message passing decoding,” *IEEE Trans. Inf. Theory*,vol. 47, no. 2, pp. 599–618, Feb. 2001.

- [10] S. ten Brink, "Convergence of iterative decoding," *IEE Electron. Lett.*, vol. 35, pp. 1117–1119, Jun. 24, 1999.
- [11] S. ten Brink, "Convergence behavior of iteratively decoded parallel concatenated codes," *IEEE Trans. Commun.*, vol. 49, no. 10, pp. 1727–1737, Oct. 2001.
- [12] S. ten Brink, G. Kramer, and A. Ashikhmin, "Design of low-density parity-check codes for modulation and detection," *IEEE Trans. Commun.*, vol. 52, no. 4, pp. 670–678, Apr. 2004.
- [13] M. Tüchler, "Design of serially concatenated systems depending on the block length," *IEEE Trans. Commun.*, vol. 52, no. 2, pp. 209–218, Feb. 2004.
- [14] A. Graell i Amat, C. A. Nour, and C. Douillard, "Serially concatenated continuous phase modulation with extended BCH codes," in *Proc. IEEE Inf. Th. Work. on Inf. Th. for Wir. Net.*, Jul. 2007, pp. 1–5.
- [15] T. L. Brandon, R. Hang, G. Block, V. Gaudet, B. F. Cockburn, S. L. Howard, C. Giasson, K. Boyle, S. S. Zeinoddin, A. Rapley, S. Bates, D. G. Elliott, and C. Schlegel, "A scalable LDPC decoder ASIC architecture with bit-serial message exchange," *Integr. VLSI J.*, vol. 41, no. 3, pp. 385–398, May 2008.
- [16] A. Darabiha, "VLSI Architectures for multi-Gbps low-density paritycheck decoders," Ph.D. dissertation, University of Toronto, Toronto, ON, Canada, 2008.
- [17] T. Mohsenin, D. Truong, and B. Baas, "A low-complexity messagepassing algorithm for reduced routing congestion in LDPC decoders," *IEEE Trans. Circuits Syst. I* [Online]. Available: <http://www.ece.ucdavis.edu/vcl/pubs/2009.11.TCAS.LDPC/ldpc.tcas.pdf>, accepted for publication
- [18] Xue Rui, Zhao Dan-feng, Xiao Chun-li "A Novel Approach to Improve the Iterative Detection Convergence of LDPC Coded CPM Modulated Signals" WICOM 2010 conference 2010
- [19] David MacKay's Gallager Code Resources [Online]. Available:<http://www.inference.phy.cam.ac.uk/mackay/codes/>
- [20] A. E. Pusane, A. Jimenez-Felström, A. Sridharan, M. Lentmaier, K. S. Zigangirov, and D. J. Costello, Jr., "Implementation aspects of LDPC convolutional codes," *IEEE Trans. Commun.*, vol. 56, Jul. 2008.
- [21] B.E. Rimoldi and Q. Li, "Coded Continuous Phase Modulation using Ring Convolutional Codes", *IEEE Tvans. Commun.*, vol. 34, pp. 2714-2720, Nov. 1995.
- [22] A. Graell i Amat, C. A. Nour, and C. Douillard, "Serially concatenated continuous phase modulation with extended BCH codes," in *Proc. IEEE Inf. Th. Work. on Inf. Th. for Wir. Net.*, Jul. 2007, pp. 1–5. *Lett.*, vol. 9, no. 2, pp. 1058–1060, Dec. 2005.
- [23] A. Sridharan and D. J. Costello, Jr., "A new construction method for low density parity check convolutional codes," in *Proc. IEEE Inf. Theory Workshop, Bangalore, India, Oct. 2002*, p. 212.
- [24] D. J. C. MacKay, "Good error-correcting codes based on very sparse matrices," *IEEE Trans. Inf. Theory*, vol. 45, no. 2, pp. 399–431, Mar. 1999.